

OROGRAPHICALLY FORCED PLANETARY FLOW**J. Egger****University of Munich, Munich, FRG**

1. Problems

We shall be concerned here with barotropic nondivergent large-scale motions on the β -plane (sphere) with orography as forcing. A 'simple' fluid system of this type is that governed by the potential vorticity equation

$$\frac{\partial}{\partial t} \nabla^2 \psi + J(\psi, \nabla^2 \psi + \frac{f_0 h}{H} + f) = -C \nabla^2 \psi + F \quad (1)$$

The notation is conventional: ψ is the stream function, h the orographic profile, $f = f_0 + \beta y$ the Coriolis parameter; H is a scale height and C is a damping constant. F stands for some kind of additional forcing. We have written our equations on the β -plane; however, most of the derivations and arguments given below need little modifications to be applicable to the sphere.

The flow will be restricted to a channel on the β -plane where the values of the stream function at the northern and southern boundary are given and do not depend on x .

Let us write

$$\psi = -u_0 y + \psi_s + \psi' \quad (2)$$

where u_0 does not depend on y or x . ψ_s is the solution of the linear inviscid steady-state mountain wave problem

$$(u_0 \nabla^2 + \beta) \psi_s + \frac{u_0 f_0 h}{H} = 0 \quad (3)$$

Let us consider flows where u_0 is constant in time (i.e. the boundary values of ψ are fixed). Neglecting for the moment F we arrive at

$$\begin{aligned} \frac{\partial}{\partial t} \Delta^2 \psi' + (u_0 \nabla^2 + \beta) \frac{\partial}{\partial x} \psi' + J(\psi', \nabla^2 \psi' + \frac{f_0 h}{H}) + J(\psi_s, \nabla^2 \psi_s + \frac{f_0 h}{H}) \\ + J(\psi_s, \nabla^2 \psi') + J(\psi', \nabla^2 \psi_s) = -C \nabla^2 (\psi_s + \psi') \end{aligned} \quad (4)$$

It is easy to prove (Egger, 1979) that

$$J(\psi_S, \nabla^2 \psi_S + \frac{f_0 h}{H}) = 0 \quad (5)$$

Then

$$\begin{aligned} \frac{\partial}{\partial t} \nabla^2 \psi + (u_0 \nabla^2 + \beta) \frac{\partial \psi}{\partial x} + J(\psi', \nabla^2 \psi' + \frac{f_0 h}{H}) + J(\psi_S, \nabla^2 \psi') \\ + J(\psi', \nabla^2 \psi_S) = -C \nabla^2 (\psi_S' + \psi') \end{aligned} \quad (6)$$

We define the mean kinetic energy

$$K = \frac{u_0^2}{2} + \frac{1}{2} \overline{(\nabla(\psi_S + \psi'))^2}^F = K_0 + K' \quad (7)$$

where $\overline{\quad}^F$ means an area average over the domain of integration. With u_0 fixed we arrive at

$$\frac{dK}{dt} = \frac{dK'}{dt} - 2CK' - \frac{u_0 f_0}{H} \overline{\frac{\partial(\psi_S + \psi)}{\partial x}}^F \quad (8)$$

The kinetic energy of the flow can increase whenever northerlies prevail over the mountains. To close the system energetically we need an additional equation for u_0 (Schilling, 1978):

$$\frac{du_0}{dt} = \frac{f_0}{H} \overline{\frac{\partial(\psi_S + \psi')}{\partial x}}^F \quad (9)$$

(damping can be included, of course)

We introduce a bar $\overline{\quad}$ as an average over time. The averaging interval should be large when compared to L/u_0 (L length of the channel). It will be helpful to discuss the flow fields in the channel in terms of Fourier modes. We shall denote the Fourier mode with zonal wave number m and meridional wave number n by (m, n) where $n-1$ is the number of zeros between the walls of the channel.

Given all that let us pose our problems:

- i) Is there a steady state for this fluid system?
- ii) Is there a time mean $\overline{\psi}$ for transient flows which does not depend on T ? Under what conditions is $\overline{\psi} \sim \psi_S$?
- iii) What kind of transient phenomena do we have to expect in such a fluid system?

Before we turn to a discussion of these problems we should perhaps briefly comment on the relevance of these questions to the large-scale dynamics of the atmosphere and to forecasting. It is

reasonable to believe that (1) portrays essential parts of the dynamics of atmospheric large-scale motions. In case we find a steady-state or at least a time mean we obtain an indication how the atmosphere or a forecast model would settle down if all the other forces and mechanisms which are not represented in (1) were turned off. In particular one would like to compare these computed mean states with the observed time means in order to see how close the atmosphere is to the purely orographically forced states.

As for the last point we shall concentrate on the blocking problem which is of obvious importance to forecasting.

2. Steady states

One might be inclined to think that (1) with $F = 0$ has a steady-state solution for the viscous case only. However, it is obvious from (6) that there exists a steady state even for the inviscid case: $\hat{\psi} = \psi_S$, $\hat{\psi}' = 0$ (where the symbol $\hat{\psi}$ denotes the steady-state solution). This result is of some interest since this solution exhibits a surprising similarity to the actual flow field in the Northern Hemisphere (at least in winter). Fig. 1 shows the observed height of the 400 mb surface in January. Fig. 1b gives the solution $\hat{\psi} = \psi_S$ of (3) with $u_0 = 25 \cos \pi / 4$ ($m \text{ sec}^{-1}$). We have included in all solutions of (3) a weak damping with $c = 1 \times 10^{-6} \text{ sec}^{-1}$ to avoid resonance effects so that the solutions presented in Fig. 1b,c are not exact solutions of the nonlinear steady-state equation. Fig. 1c gives the solution of (3) where the zonal flow corresponds to a superrotation. Fig. 1d has been obtained by solving the linear standing wave vorticity equation corresponding to (3) on the sphere but with realistic January mean wind. In that case we cannot claim that the linear solution is also a solution of the nonlinear problem. The standing waves in Fig. 1 b-d are grossly exaggerated as compared to the observations since we did not use a reduction factor for the mean wind in the mountain forcing term. However, all our solutions show the large-scale troughs over Canada and North-East Asia as well as the observed ridges over the Pacific and Atlantic. The January

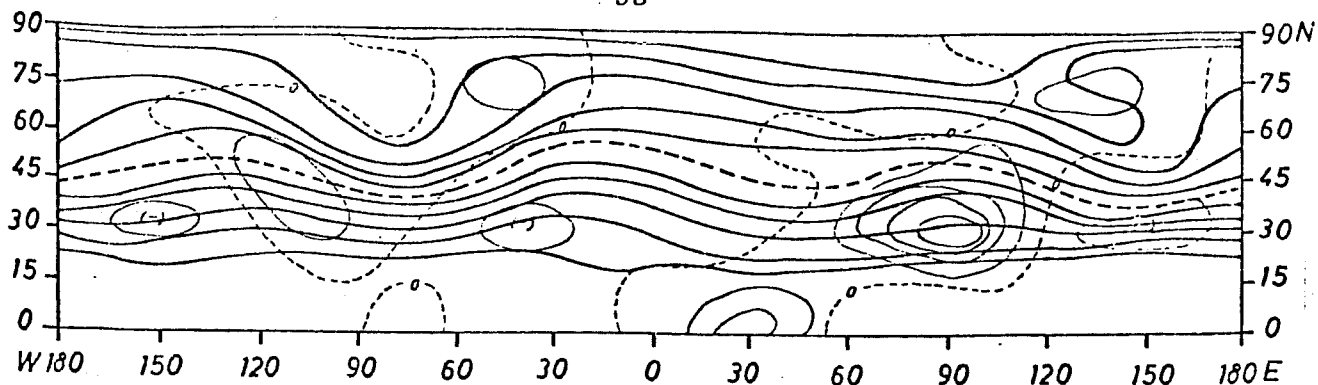


Fig.1a. The observed height of the 400 mb surface in January, with isolines every 100 m and 7000 m contour dashed (after Gates , 1972). The thin lines represent the orography with isolines every 100 m and the 0 m contour dashed.

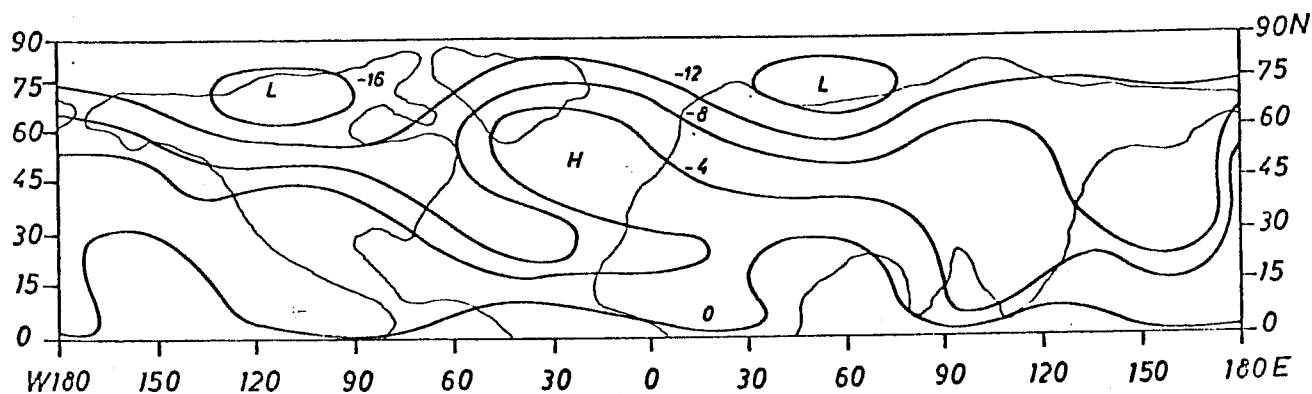


Fig.1 c - d. Solutions of the steady-state linearized potential vorticity equation with orography of the Northern Hemisphere. The equation is solved by using grid points between equator and pole and a Fourier representation in longitude with six zonal wave numbers. We display the geopotential ($100 \text{ m}^2 \text{ sec}^{-2}$) of the sum of the prescribed zonally averaged state and the orographically forced perturbations. The geopotential is related to the computed stream function via $f\psi = \phi$. Fig.1 b gives the β -plane solution of (3) with $u_0 = 25 \cos \pi / 4 \text{ m sec}^{-1}$.

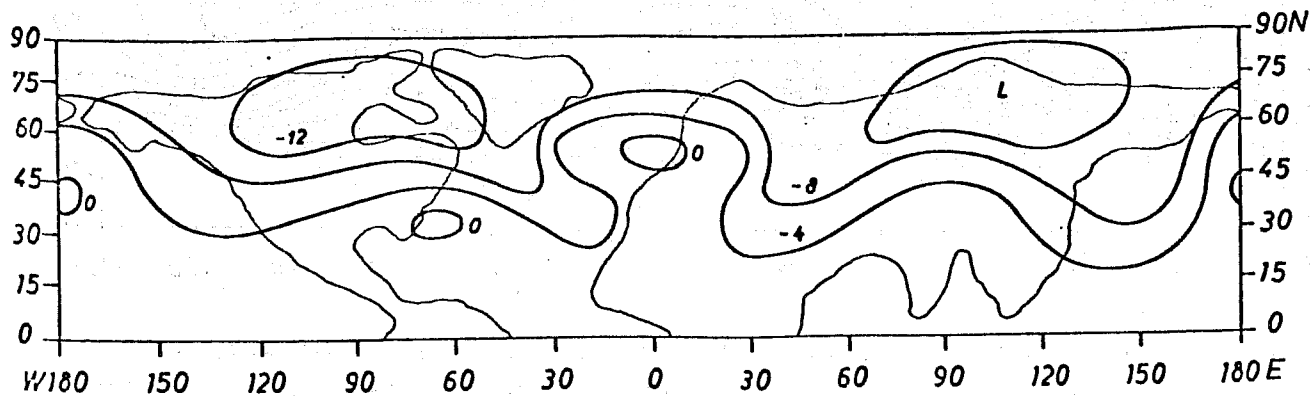


Fig.1c. Solution of (3) on the sphere with $u_0 = 25 \cos \sigma \text{ m sec}^{-1}$

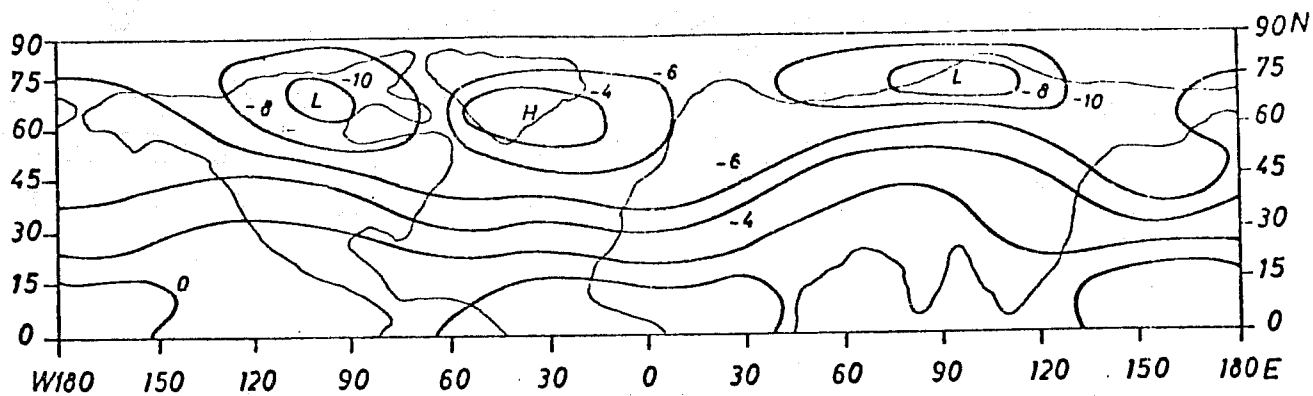


Fig.1 d. Observed January zonal mean flow at 400 mb.

solution appears to be the most realistic one. Note the blocking flow pattern over the Atlantic in Fig.1b and, somewhat blurred, in Fig.1c and d. Our results are in qualitative agreement with the linear steady-state solutions of the shallow water equations presented by Grose and Hoskins (1979) and, of course, with the pioneering paper by Charney and Eliassen (1949) who got quite satisfactory coincidence with the observations by using an almost one-dimensional version of (3). In particular, the occurrence of blocking patterns has been found by Grose and Hoskins as well.

The coincidence between Fig.1b and the observations suggests that the steady state solution $\hat{\psi} = \psi_s$ is approached to some extent by the atmosphere. It would be interesting to look into the stability of this steady-state. This is left for future work.

Before we turn to the fully viscous case it might be worthwhile to have a brief look at the situation in oceanography. Bretherton and Haidvogel (BH; 1976) studied the evolution of 'almost inviscid' flow above topography in a closed basin in an attempt to deal with the characteristics of meso-scale eddies in the ocean. They used (1) but with a fourth-order diffusion thus restricting the dissipation to the largest wave-numbers. They found in experiments on the f-plane that a very nearly steady-state could be achieved where the vorticity became strongly anti-correlated with the topography (Fig.2). The final state displayed stream lines parallel to the contours of constant depth, anti-cyclonic around mountains. BH argued that the enstrophy in two-dimensional flow cascades towards the smallest scales at which it is dissipated whereas the kinetic energy K goes towards the largest scales and remains almost constant. Then one has to expect a steady state of the form

$$\nabla^2 \hat{\psi} \frac{f_0 h}{H} = \mu \hat{\psi} \quad (10)$$

where μ is linked to K . Once β got included the result depended on the energy of the initial state. With relatively large initial energy a steady state was reached where again topography and vorticity were anticorrelated whereas the total energy fell rather rapidly for low initial energies.

What kind of results would have been obtained by BH if they would have run their model with our boundary condition? Normally their arguments

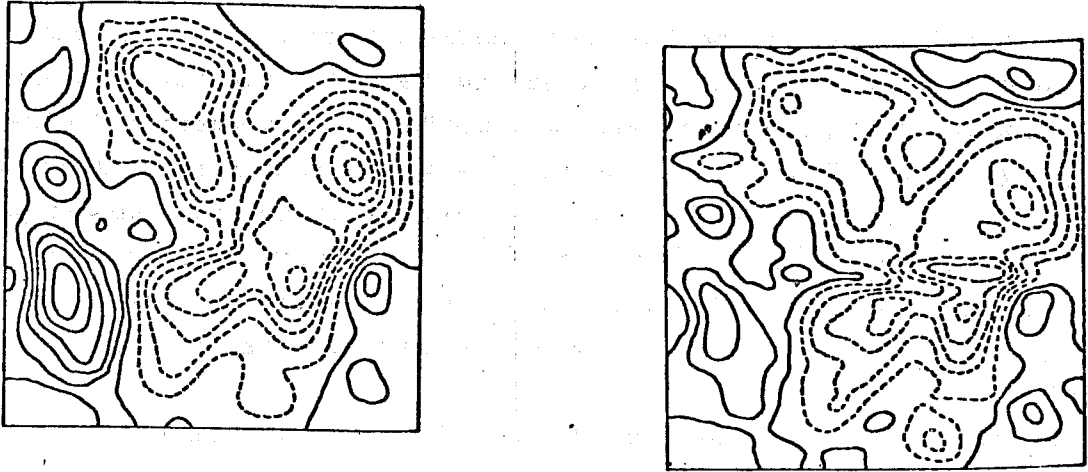


Fig.2. Topography (left) and steady-state stream function in the f -plane experiment of BH. Dimensionless units. Redrawn from Fig.2 of BH.

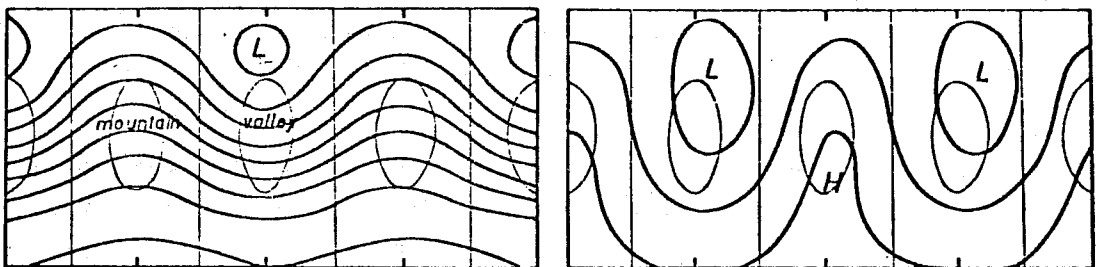


Fig.3. Stream function of the two steady states found by Charney and de Vore. The thin lines give the position of the topography. Dimensionless units. Redrawn from Fig.3 of Charney and de Vore.

would not be valid in our case since K has a source (see (8)). However, this source term would vanish for $u_0 = 0$. Then , the arguments of BH would lead to an equation for the steady state

$$\nabla^2 \psi + \frac{f_0 h}{H} + \beta y = \mu \psi \quad (11)$$

where μ is linked to K . It is easy to see that we would have to expect a zonal mean flow which changes direction in the channel. It is, however, not so easy to see what the correlation between orography and vorticity would be. We shall not present such an analysis . This is partly because we do not have a high-resolution model for turbulent flows like BH so that we cannot test such hypotheses. Secondly, neither the absence of friction at the largest scales nor the vanishing of u_0 are realistic assumptions for atmospheric large-scale flow.

The numerical experiments to be described in this paper have been carried out with a rather severely truncated spectral model where typically $m \leq 5$, $n \leq 3$. Charney and de Vore (1979) looked into the steady-state problem for such simplified flow systems. They integrated the shallow water equations in a channel with a one-mode topography and linked their results to an analysis of a four-mode solution of (1). They prescribed a simple driving mechanism for the zonal flow and had a damping as in (1). They found that the flow system possessed two stable steady states under favorable conditions (Fig.3). The one is characterized by anti-cyclonic flow above the valleys, the other by anticyclonic flow above the topography similar to the BH solution. The one exhibits a relatively weak standing wave at the same mode as the orography whereas the other one shows strong waves at the second meridional mode of the channel. Similar results have been obtained in an analytic study by Buzzi and Trevisan (1979). Such results suggest that the existence of different types of persistent Großwetterlagen may be associated with the multiplicity of orographically forced steady states.

In an attempt to see what happens when the orography is more realistic than in the case of Charney and de Vore, I have integrated (1) in a channel with walls at 15°N and 75°N and with the orography of the Northern Hemisphere. A value of $u_0 = 14 \text{ m sec}^{-1}$ has been chosen which made the mode (2,2) 'resonant'. With $C = 1 \times 10^{-6} \text{ sec}^{-1}$ and an arbitrary

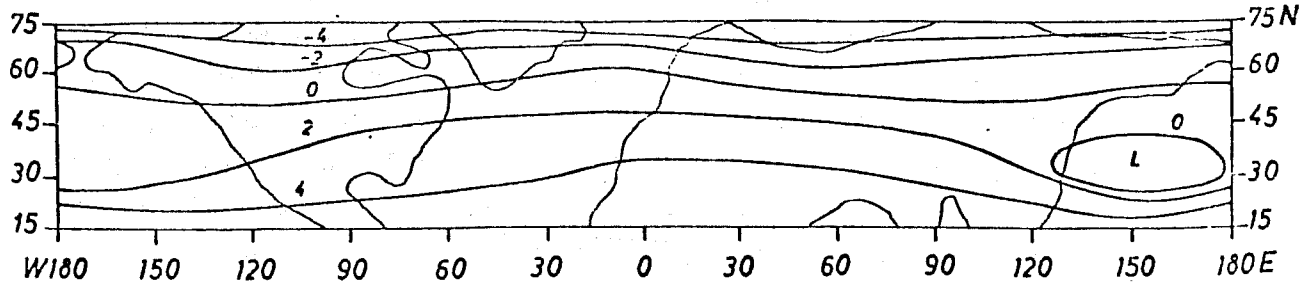


Fig.4. Stream function of the steady state ($10^7 \text{ m}^2 \text{ sec}^{-1}$). $C = 1 \times 10^{-6} \text{ sec}^{-1}$. B-plane; realistic orography; $m \leq 3$, $n \leq 3$.

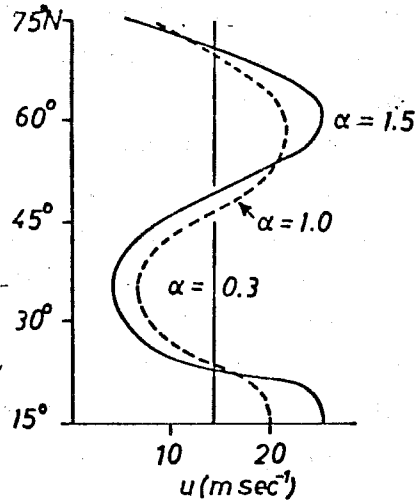


Fig.5. Meridional profile of the zonally averaged wind of the steady-state solutions ϕf (1) with $\alpha = 0.3, 1.0, 1.5$ resp..

initial field we arrive at a very nearly steady state after, say, 30 days. (Fig.4). Comparing this steady state with Fig.1b we find that the fields are much smoother now. The only obvious coincidence occurs off Asia where we find a well developed trough in both solutions. The large deviations between Fig.1b and Fig.4 suggest that nonlinear terms play a dominant role in maintaining the viscous steady state.

To get a feeling for the intensity of the nonlinear interactions we have repeated the run but changed the height of the orography by a factor α . The less α the closer we should come to the linear solution ψ_S (corrected to include friction). Tab.1 gives the Fourier coefficients of the modes (1,1), (2,1), (3,1) and (2,2) for experiments with $\alpha = 0.3, 0.7, 1.5$ resp. as well as the solution of the linear problem.

We see that the steady state for $\alpha = 0.3$ is fairly close to the linear solution except for the mode (2,2) and for the cosine of (1,1). The latter failure is probably due to the weak forcing whereas the deviations at (2,2) are explained by the fact that the Rossby phase velocity $c_{22} \approx 0$. We cannot expect to get standing waves in agreement with the linear theory for such a slow mode. Once we increase α to 1.5 the coincidence with the linear theory becomes rather poor. Hence, the steady-state solution for such a strong forcing shows a decidedly nonlinear character. This is also demonstrated in Fig.5 where the profiles of the zonal wind are displayed. For $\alpha = 0.3$, $u \sim u_0$ whereas strong shear is seen for $\alpha = 1.5$.

A search for another steady state has been undertaken by starting numerical experiments from $\psi = -u_0 y + \psi_S$, $\alpha = 1$. However, these runs converged towards the steady state displayed in Fig.4.

It could have been anticipated that a system like ours with forcing and dissipation has a steady state for certain areas in the parameter space. However, it is surprising that the inviscid steady state is so close to the observed mean flow. This is the more surprising since this steady state differs considerably from that obtained with $C = 1 \times 10^{-6} \text{ sec}^{-1}$. Note that the latter steady state is rather different from that predicted by BH. There is no coincidence between orography and vorticity but we have a systematic phaseshift between ψ and h to make $h \frac{\partial \psi}{\partial x} < D$ and to have a balance of the dissipation.

Mode	(1, 1)	(2, 1)	(3, 1)	(2, 2)
1. $\alpha = 1$. Linear solution with friction	0.7/ 3.0	7.2/-3.3	1.7/-3.6	-7.6/-11.2
2. $\alpha = 0.3$	-0.1/1.1	2.3/-0.6	0.7/-1.0	2.3/3.4
3. $\alpha = 0.7$ steady-states	-3.5/3.5	3.7/1.9	1.8/0.9	0.6/9.8
4. $\alpha = 1.5$	-9.7/ 2.2	4.1/1.7	-0.2/0.8	4.6/6.0
5. Rossby phase speed $c_{mn} = u_0 - \beta/kmn^2$	- 43	-22	-9	0

Tab1. Fourier coefficients (cos/ sin) of various modes in $10^6 m^2 sec^{-1}$.

1. Linear solution with $u_0 = 14 m sec^{-1}$. 2-4. Computed steady states with various values of α . 5. Rossby phase speed of the modes in $m sec^{-1}$.

Mode	(1,1)	(1,2)	(1,3)	(2,1)	(2,2)	(2,3)	(3,1)	(3,2)	(3,3)
T_L / T_N	-0.5/8	-5.2/2.4	1.1/1.1	-0.2/5.4	0.0/2	1/1	-1.5/3.4	3.7/1.7	0.9/0.9

Tab.2. T_L and T_N for various modes (days).

The existence of multiple steady states is another exciting result. It is, on the other hand, rather obvious that these results are quite isolated and that we do not have a comprehensive theory of the steady states of orographically forced flows.

3. Transient flows.

Given an initial state different from ψ_s and a sufficiently small value of the solution of (1) will not tend towards a steady state. If $|\psi'| \leq |\psi_s|$ one would expect $\bar{\psi} \sim 0$ and $\bar{\psi} \sim \psi_s$ since in that case $J(\psi', \nabla^2 \psi')$ should be of minor importance when compared with the 'linear' term $(U_0 \nabla^2 + \beta) \frac{\partial \psi}{\partial x}$.

A good example for such weakly nonlinear flows has been provided by Kasahara (1967). He solved the inviscid shallow water equations on the sphere starting from a zonally averaged initial state which corresponded to the observed 500 mb state in January. He ran his model for 20 days. Fig.6 shows a mean over the last 15 days (small T). Comparing Fig.6 to Fig.1d we note a fairly good coincidence between the linear steady state solution and Kasahara's finding. We have prominent troughs in the lee of the Rockies and of the Himalaya in both figures. In general, the oceans are high pressure areas. Qualitatively speaking $\bar{\psi} \sim \psi_s$ in Kasahara's experiment.

However, we have to be cautious against drawing this conclusion. First, Kasahara did not run his model long enough to make sure that a meaningful time mean has been established. Second our guess that $(U_0 \nabla^2 + \beta) \frac{\partial \psi}{\partial x} - J(\psi', \nabla^2 \psi')$ will hold only for those modes with a sufficiently large phase speed.

Given a mode (m,n) we may define a linear time

$$T_{Lmn} = (K_{mn} C_{mn})^{-1} \quad (12)$$

where k_{mn} is the wave number. Similarly a nonlinear time

$$T_{Nmn} = (\psi^0 K_{mn}^2)^{-1} \quad (13)$$

may be defined which is characteristic of the nonlinear interactions (e.g. Egger, 1978). ψ^0 stands for the amplitude of the x-dependent Fourier modes in the channel. We can expect to find $\bar{\psi}_{mn} \sim \psi_{mns}$ for those

modes where $T_N/T_L \gg 1$. Tab.2 gives T_L and T_N for various modes in a channel corresponding to that shown in Fig.4. Obviously there are a number of modes where $T_N \sim T_L$. Longterm experiments with such a flow will lead to $\bar{\psi} \sim \psi_S$ at best for those modes with $T_N / T_L \gg 1$. The other modes will be dominated by nonlinear interactions.

It is, however, difficult to thoroughly test these ideas. As long as we treat u_0 as a constant there is no energy conservation for inviscid flow. We are well informed about the relevant linear and nonlinear times but we cannot expect to find meaningful time averages. As a matter of fact K grew in all such experiments (despite an energy conserving numerical scheme).

One way to get around this difficulty is to put $u_0 = 0$. The experiment has been made and it turned out that $\bar{\psi}' \sim 0 \sim \psi_S$. A similar result has been obtained by Metz (1979) who integrated (1) on the sphere with vanishing superrotation. Of course $\bar{\psi}' = 0$ is a solution of the time averaged equation (1) with $u_0 = 0$:

$$\beta \frac{\partial \bar{\psi}'}{\partial x} + J(\bar{\psi}', \nabla^2 \bar{\psi}') + \frac{f_0 h}{H} = -C \nabla^2 \bar{\psi}' \quad (13)$$

whenever the transient eddies do not transport transient vorticity:

$J(\bar{\psi}', \nabla^2 \bar{\psi}') \approx 0$. Another method to solve this problem would be to add (9) which ensures a conservation of the total energy of the flow. Once we do that u_0 drops rather rapidly (Fig.7). At first this is not a surprising result since the waves contained no energy at $t = 0$. Therefore, u_0 has to drop in order to provide energy for the orographically induced waves. However, u_0 came even close to zero in 'equilibrium' when the resolution of the model was increased. Furthermore, u_0 reached the same 'equilibrium' value as in Fig.7 when its initial value was 30 m sec^{-1} .

We speculate on the basis of this rather limited number of experiments that barotropic flows with orography are in equilibrium only for $u_0 \sim 0$, provided the orography is strong enough and the resolution is sufficient. With $u_0 \sim 0$, $T_L \ll T_N$ and we would expect to have Rossby waves in the channel which hardly interact.

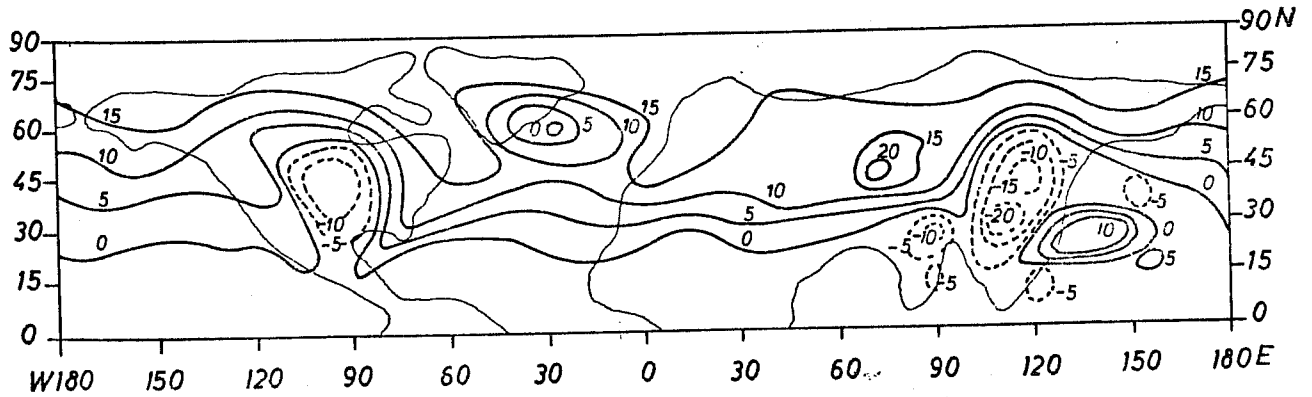


Fig.6. Mean deviation of the height of the free surface in decameters as found by Kasahara (1966) . We show here only the part of Kasahara's result which is situated in the Northern Hemisphere.

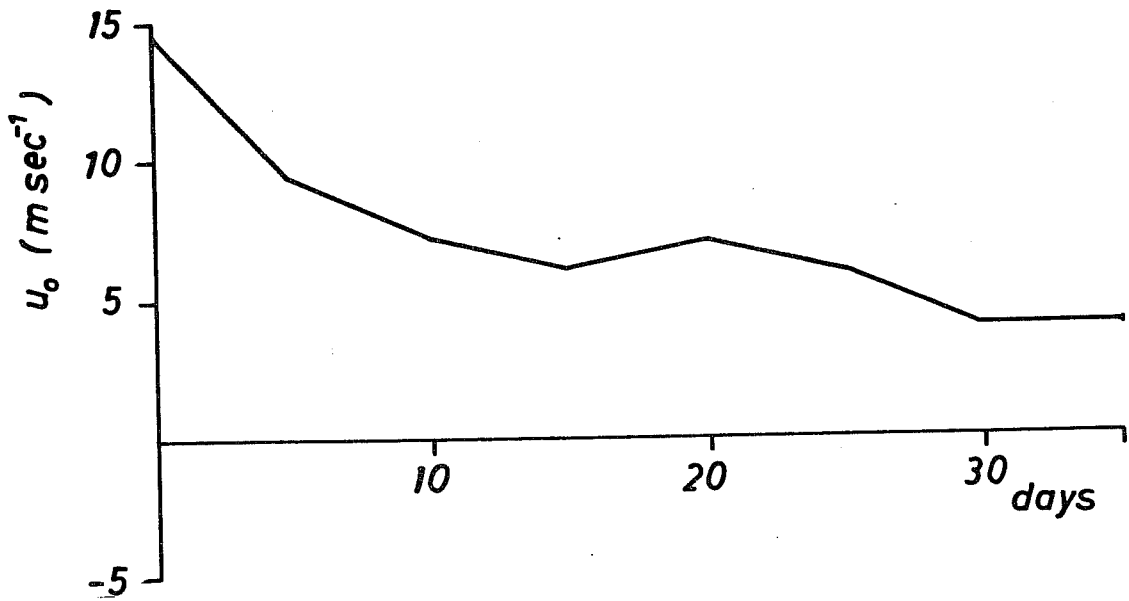


Fig.7. u_0 as a function of time in an inviscid run on the β -plane.

Finally, one can try to find a value of C suitable to balance the orographically enforced increase of energy. For example, with $C = 0.5 \times 10^{-6} \text{ sec}^{-1}$ K grew from $150 \text{ m}^2 \text{ sec}^{-2}$ to 210 during 50 days.

It is reasonable to talk about time means in such a experiment. Fig.8 shows the Fourier coefficients of the mode (2,2) in time.

$\psi_{22} = 0$ initially. We observe a linear growth during the first days which can be shown to be due to the mountain forcing of this mode. This development comes to a halt rather soon since friction is coming into effect. However, ψ_{22} never reaches the equilibrium between damping and mountain forcing since the interaction with other modes produces slow changes off the linear equilibrium. We get $5 (8) \times 10^6 \text{ m}^2 \text{ sec}^{-1}$ for the time mean of the cosine (sine) coefficient of . The linear theory yields $\bar{\psi}_{22} = 1.5 (2) \times 10^6$. It is worth noting that not even the mode (1,1) comes close to the value predicted by the linear theory when averaged over the 50 days.

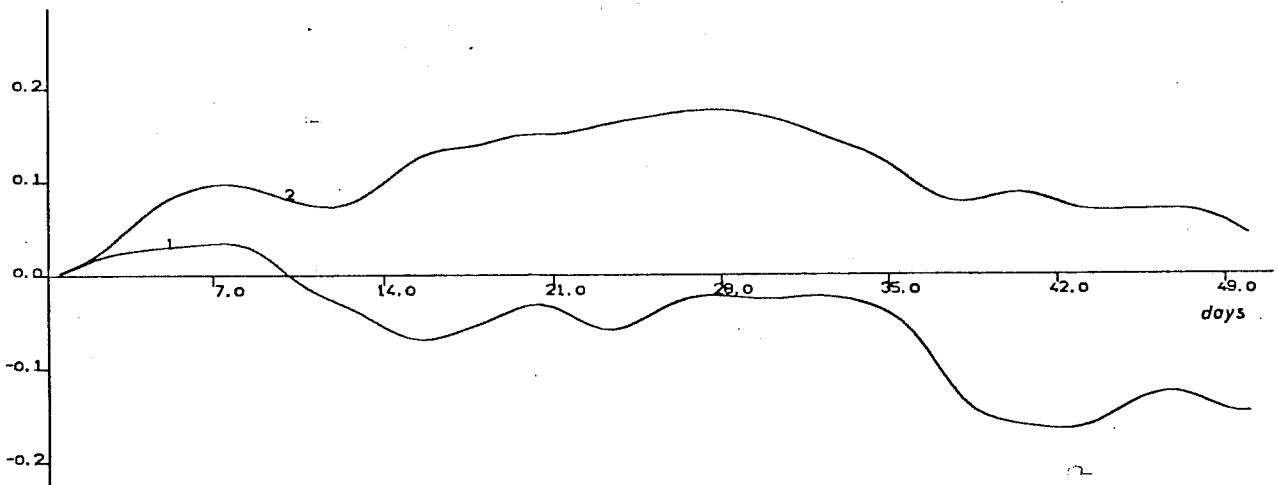
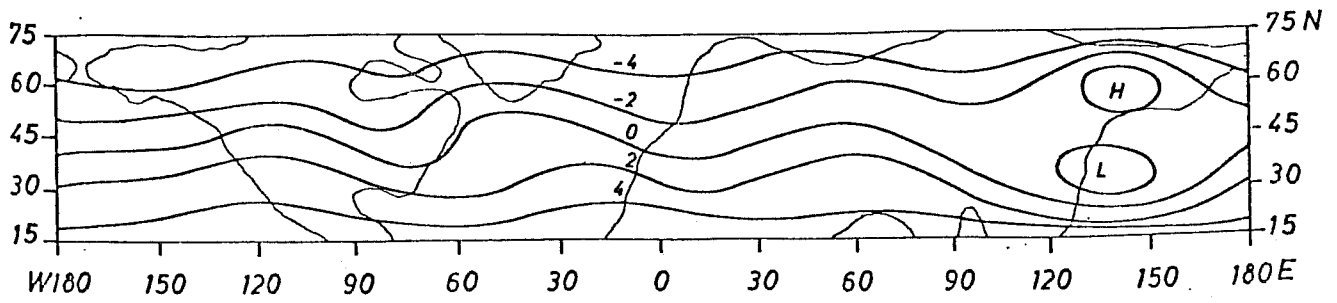
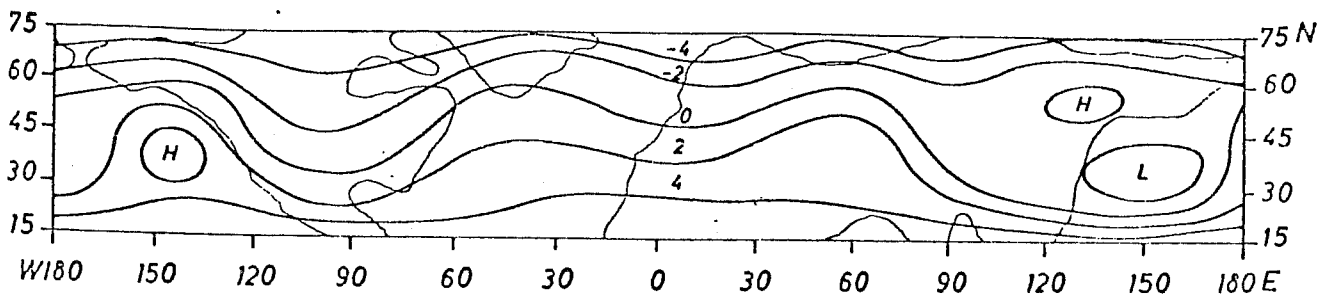


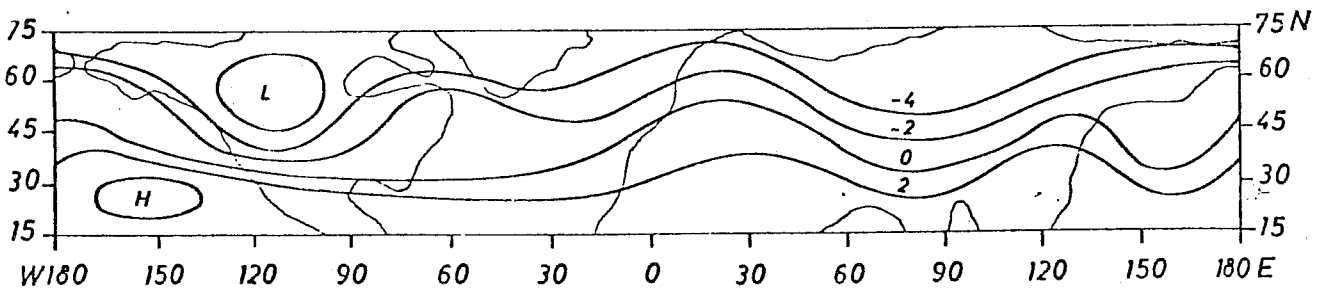
Fig.8. Development of the Fourier coefficients (1= cosine, 2 = sine, $10^7 \text{ m}^2 \text{ sec}^{-1}$) of the mode (2,2) in an experiment with $u_0 = 14 \text{ m sec}^{-1}$, $m \leq 5$, $n \leq 3$, $C = 0.5 \times 10^{-6} \text{ sec}^{-1}$; β -plane.



a)



b)



c)

Fig.9. Stream function ($10^7 \text{ m}^2 \text{ sec}^{-1}$) at day 7 (a), 10 (b) and 25 (c) of a channel flow experiment with $C = 0.3 \times 10^{-6} \text{ sec}^{-1}$, $m \leq 5$, $n \leq 3$, $u_0 = 14 \text{ m sec}^{-1}$. Orography of the Northern Hemisphere but changed to have $h = 0$ at the walls. The orographic mode (1,1) is missing for reasons which have nothing to do with the objectives pursued here.

In conclusion one might try to answer ii) by saying that $\bar{\psi} \sim \psi_s$ as long as $T_L \ll T_N$ for most of the dominant modes of the flow. It is not clear what happens when it is otherwise. On the other hand, it became obvious during the foregoing that it is difficult to produce solutions of (1) with $u_0 \neq 0$ which have a reasonable time mean state (at least as long as $F = 0$).

Finally, let us look at transient features of the flow fields. It has been shown (Egger, 1979) that orography at two modes can induce blocking. Let us turn here towards a more realistic orography. Fig.9 shows flow patterns obtained with the orography of the Northern Hemisphere as forcing. Starting with vanishing wave amplitudes we obtain a rather fine blocking pattern near 140° E at day 7 which drifts slowly towards the east. The block has a life time of about 10-12 days and can't be seen any more at day 25. On the other hand, there is quite a similarity of all the fields shown in Fig.9. With other words, our flow doesn't show much transiency and is rather close to a steady state. Then, it is not really surprising that we can create blocks in such a run since we have seen that blocking patterns can be found even in linear steady state solution. We have repeated the run but excluded the wave-wave interactions. It turned out that the pattern at day 7 and day 10 were rather similar to those displayed in Fig.9. Hence we can state that blocking flow patterns can be created by orography in almost linear flow systems.

On the sphere the results are almost the same. As already mentioned, Metz (1979) has integrated (1) on the sphere for about 100 days starting from a purely zonal flow field with $u = 17 \cos \phi$, $C = 0$. Several blocking patterns formed with a clear preference for the Pacific and the Atlantic areas. Fig.10 shows an example of such a block. We have the familiar high-low system above the Atlantic with a well developed split of the jet to the west. Again, a run with wave-wave interactions excluded gave similar blocks.

We feel, however, that it would be premature to conclude from these experiments that blocking is an essentially linear phenomenon caused by orographic forcing. We have to bear in mind that the models used here truncate the wave spectrum rather severely and exclude baroclinicity. Furthermore additional experiments with the models are required to more clearly elucidate the blocking process in the models.

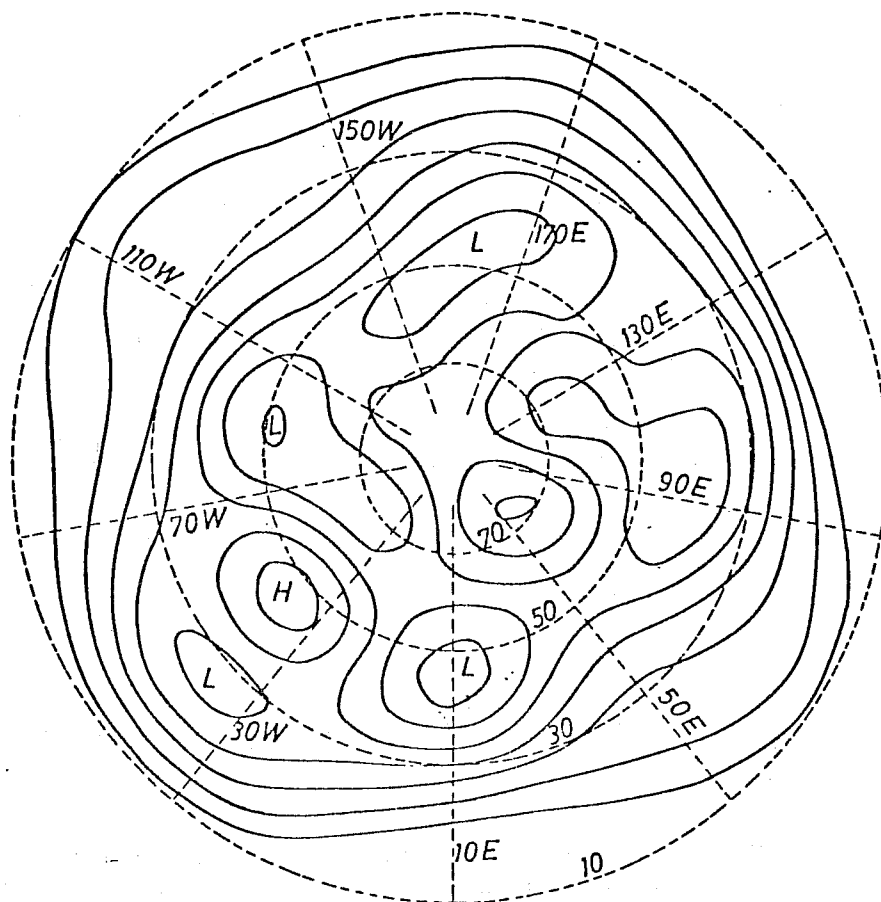


Fig.10. Geopotential at day 51 of an integration of (1) on the sphere with orography of the Northern Hemisphere. $C = 0$. After Metz (1979).

References

- Brotherton, F. and D. Haidvogel, 1976: Two-dimensional turbulence above topography. J.F. Mech. 78, 129-154.
- Buzzi, A. and A. Trevisan, 1979: Personal communication.
- Charney, J. and A. Eliassen, 1949: A numerical method for predicting the perturbations of the middle latitude westerlies. Tellus 1, 48-54.
- Charney, J. and J. de Vore, 1979: Multiple flow equilibria in the atmosphere and blocking. To be published.
- Egger, J. 1978: Dynamics of blocking highs. J. Atmos. Sci. 35, 1788-1801.
- Egger, J. 1979: Stability of blocking in barotropic channel flow. Beitr. Phys. Atmos. 52, 27-43.
- Gates, W. 1972: The January global climate simulated by the two-level Mintz-Arakawa model: a comparison with observations. RAND, Santa Monica.
- Grose, W. and B. Hoskins, 1979: On the influence of orography on large-scale atmospheric flow. J. Atmos. Sci. 36, 223-234.
- Kasahara, A. 1967: The influence of orography on the global circulation patterns of the atmosphere. Proc. Symp. Mount. Met. Fort Collins, Colorado. R. Reiter and J. Rasmussen, editors.
- Metz, W. 1979: Blocking on the sphere. Unpublished manuscript. Schilling, D. 1978: Personal communication.